



HAL
open science

Active Robust Fault Estimation on a Composite Beam with Integrated Piezoceramics

Nazih Mechbal, Michel Vergé

► **To cite this version:**

Nazih Mechbal, Michel Vergé. Active Robust Fault Estimation on a Composite Beam with Integrated Piezoceramics. 6th IFAC Symposium on Fault Detection, Supervision and Safety of Technical Processes (SAFEPROCESS'06), 2006, Pekin, China. 10.3182/20060829-4-CN-2909.00198 . hal-00292240

HAL Id: hal-00292240

<https://hal.science/hal-00292240v1>

Submitted on 15 Apr 2023

HAL is a multi-disciplinary open access archive for the deposit and dissemination of scientific research documents, whether they are published or not. The documents may come from teaching and research institutions in France or abroad, or from public or private research centers.

L'archive ouverte pluridisciplinaire **HAL**, est destinée au dépôt et à la diffusion de documents scientifiques de niveau recherche, publiés ou non, émanant des établissements d'enseignement et de recherche français ou étrangers, des laboratoires publics ou privés.



Distributed under a Creative Commons Attribution 4.0 International License

ACTIVE ROBUST FAULT ESTIMATION ON A COMPOSITE BEAM WITH INTEGRATED PIEZOCERAMICS.

N. Mechbal¹ & M. Vergé

*Laboratoire de Mécanique des Structures et des Procédés (LMSP – UMR, CNRS)
École Nationale Supérieure des Arts et Métiers (ENSAM, Paris).
151, Boulevard de l'Hôpital, Paris, France.*

Abstract: The problem addressed here is the application of model-based fault detection algorithm to active control of flexible structures. The modeling of mechanical structures with the finite element (FE) method leads to high order models which must be reduced. This step introduces important uncertainties which make necessary the use of robust fault detection and diagnosis (RFDD) algorithms. Here, we propose to apply a RFDD method using the H_2 and H_∞ polynomial estimation to estimate the input fault signal. To illustrate the efficiency of this method, it is applied to a composite beam with piezoelectric patches. as sensors and actuators.

Keywords: Active control, Fault estimation, Robustness, Finite Elements, H_2/H_∞ polynomial estimation, Piezoceramics.

1. INTRODUCTION

Suppression of vibrations has received a great interest in the recent years. In the past decade, active control of vibrations has emerged as a viable technology. It has shown a great efficiency in comparison with passive damping. Its developments have been propelled by the rapid technology growth in practical digital signal processing and by the use of smart materials with adaptable properties such as piezoelectric ceramics.

The smart structure obtained is able to react to external perturbations. But it is also more sensitive to the failure of any element (e.g. actuators, sensors or onboard electronics). In fact, due to wear of mechanical and electrical components piezo-ceramics might fail in more or less critical way (for example, cracks can appear in the ceramics). As a consequence, procedure of fault detection and diagnosis (FDD) is necessary to ensure reliable and safe operating.

Fault detection and diagnosis methods have been the subject of intensive investigation over the past two decades. Most of studies concern analytical redundancy management. Several methods have been

presented using alternative approaches like the parity relations, observers and eigenstructure assignment approaches. A useful and recent survey is given by Iserman (2005). Furthermore, the FDD procedures have to be robust to exogenous inputs, noises and failure mode modeling errors. Hence, they should be able to separate the effect of model uncertainties and perturbation from the effect of failures.

In active control, the goal is to design a feedback controller that increases the system damping (Gawronski, 1998). Moreover, the necessary step of FE model reduction, introduces important uncertainties, which added to the fact that stiffness and natural frequencies can only be approximated, make necessary the use of robust control and also fault detection algorithms.

In this contribution, we propose to apply the original method developed by Mechbal and Vergé (2001) to active fault detection on a minimum phase plant. The method is based on robust H_2 and H_∞ polynomial estimators. In this approach, the robust detection problem is reformulate in a problem of robust estimation, where the unmeasured signal to be estimate is the input fault signal. The flexible structure under study is a composite beam with piezoelectric patches. To perform classical linear dynamical analyses we use *Nastran* software with an original approach elaborated by Mechbal (2005).

¹ Corresponding author.

Tel. +33-1-44-24-64-58; Fax: +33-1-45-86-62-63

E-mail address: Nazih.Mechbal@paris.ensam.fr

The polynomial approach to H_2 and H_∞ estimation and control problem was first introduced by Kwakernaak (1986) and developed in a discrete-time context by Grimble (1993). This method, whose importance was recognized, for its role in signal processing and robust control problems, has been used in a fault detection context by Mechal et al. (2000, 2001).

The paper is organized as follows. Section 2 is devoted to a description of the system under consideration and the fault model. In Section 3 and 4, we review the polynomial estimation problem and the H_2 and H_∞ optimal fault detectors. In Section 5, after a description of the active structure, the FE model and experimental results are presented.

2. DESCRIPTION OF THE SYSTEM

In this paper we are concerned with the analysis of linear discrete-time, stationary stochastic models in the standard transfer function form. To be simple, here, we restrict our study to SISO systems.

Consider now the class of systems described by Fig. 1. Signal $d(k)$ represents an input perturbation and signal $b(k)$ stands for a colored measurement noise. The two noises sources $\zeta(k)$ and $\omega_b(k)$ are time-invariant, mutually independent with zero means, and their covariance are defined respectively as $\text{cov}[\zeta(k), \zeta(l)] = Q_d \delta_{kl}$ and $\text{cov}[\omega_b(k), \omega_b(l)] = Q_n \delta_{kl}$. Here δ_{kl} denotes the Kronecker delta function. All subsystems involve only polynomial terms in the indeterminate z^{-1} and are represented by the following coprime representation:

$$\begin{aligned} W(\theta, z^{-1}) &= A(z^{-1})^{-1} B(z^{-1}) \\ W_d(\theta, z^{-1}) &= A_d(z^{-1})^{-1} C_d(z^{-1}) \\ W_b(z^{-1}) &= A_b(z^{-1})^{-1} C_b(z^{-1}) \end{aligned} \quad (1)$$

We assume the noise model is stable. The observation signal is then given in the no faulty case by

$$z(k) = W(z^{-1})u(k) + W_d(z^{-1})\zeta(k) + W_b(z^{-1})\omega_b(k) \quad (2)$$

In our fault detection context, the effect of faults on system dynamics is modeled (Fig.1) by one additive faulty signal $f(k) \in \mathfrak{R}^q$ on the output that comes from the contribution of several fault signals as using a shaping filter $f_i(k)$, i.e.

$$f(k) = \sum_i f_i(k) \quad i = 0, \dots, q.$$

Moreover, in order to successfully identify individual fault we assume that each faulty signal $f_i(k)$ is described using a shaping filter:

$$f_i(k) = W_{f_i}(z^{-1})\varepsilon_{f_i}(k) \quad (3)$$

where $W_{f_i}(z^{-1}) = A_f^{-1}(z^{-1})C_f(z^{-1})$ denotes a stable minimal weighting function and $\varepsilon_{f_i}(k)$ signal that is anticipated to have flat power spectrum.

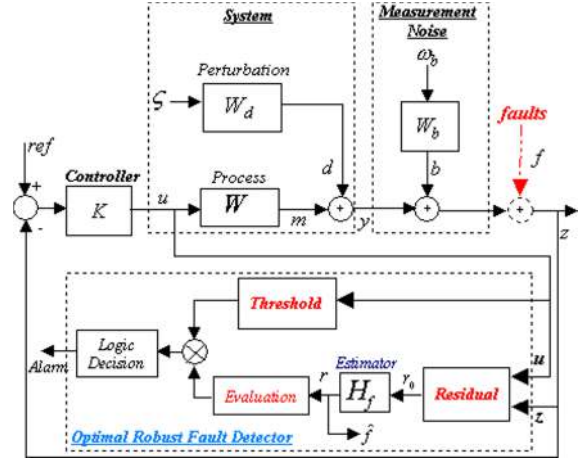


Fig. 1: The feedback system and the optimal fault detector.

It's a fictitious signal with the sole purpose of generating the frequency colored signals f_i . In the stochastic context, we suppose that each ε_{f_i} is a zero mean white noise with identity covariance. Observation signal is now given in the faulty case by

$$\begin{aligned} z(k) &= m(k) + d(k) + b(k) + f(k) \\ &= W(z^{-1})u(k) + W_d(z^{-1})\zeta(k) + W_b(z^{-1})\omega_b(k) \\ &\quad + W_f(z^{-1})\varepsilon_f(k). \end{aligned} \quad (4)$$

3. OPTIMAL FAULT DETECTOR

The goal here is to show how the H_2 and H_∞ polynomial estimation can be used to generate optimal residuals that provided us an estimation of the fault.

Notations: We denote $\hat{x}(k)$ the estimate of the unmeasured signal $x(k)$. We also denote $A^*(z^{-1})$ the self-adjoint of the polynomial $A(z^{-1})$, i.e. $A^*(z^{-1}) = A(z)$. To simplify the notation, the dependence upon z^{-1} is omitted from now on.

3.1. Residual generation

First, we introduce the following spectral factorization:

$$Y_s Y_s^* = W_d Q_d W_d^* + W_b Q_b W_b^* \quad (5)$$

The spectral factor Y_s can be represented in a polynomial form as $Y_s = A_s^{-1} D_s$, where A_s and D_s are Schur polynomials derived from the following factorization

$$\begin{aligned} D_s D_s^* &= \tilde{C}_d Q_d \tilde{C}_d^* + \tilde{C}_b Q_b \tilde{C}_b^* \\ A_s^{-1} \begin{bmatrix} \tilde{C}_d \\ \tilde{C}_b \end{bmatrix} &= \begin{bmatrix} A_d^{-1} C_d \\ A_b^{-1} C_b \end{bmatrix} \end{aligned} \quad (6)$$

As mentioned earlier, the useful signals for the residual generation are the known input vector and the measurable output. Therefore, without loss of generality, we define from (2) the stable residual by

$$r(k) = H_f(z(k) - Wu(k)) = H_f r_0(k) \quad (7)$$

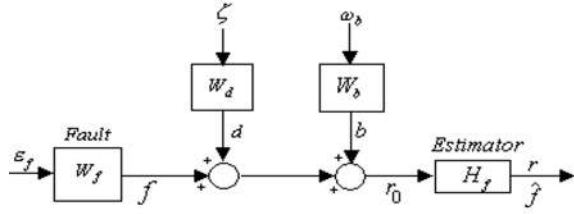


Fig. 2: Fault estimation.

where H_f is an optimal filter to be determined. In the case where the system is unstable a stable residual generator is always available by using coprime factorization (Grimble, 1993). We assume now that all the subsystems in (1) are stable. Hence, using (7), (2) and in the no faulty case, the measured signal r_0 can be rewritten in the innovation form as,

$$r_0(k) = W_d \zeta(k) + W_b \omega_b(k) = A_s^{-1} D_s \xi(k) \quad (8)$$

where $\xi(k)$ denotes white noise of zero mean with unity covariance.

Suppose now that a fault $f(k)$ occurs. This fault will alter the behavior of the system and the residual will be given by:

$$\begin{aligned} r(k) &= H_f(r_0(k) + f(k)) \\ &= H_f(A_s^{-1} D_s \xi(k) + A_f^{-1} C_f \epsilon_f(k)) = H_f r_f(k). \end{aligned} \quad (9)$$

The filter H_f is determined in order to make the influence of disturbance as small as possible while keeping the fault signal as large as possible. To solve this problem, Mechbal and Vergé (2001) proposed a method that transform the problem of detection to an estimation problem where now the unmeasured signal to be estimated is the fault (Fig. 2). Hence, the goal is to find the best estimate $\hat{f}(k)$ of $f(k)$ in the presence of the perturbation signal $r_0(k)$. For, we define the following estimation error:

$$e_f(k) = (f(k) - \hat{f}(k)) \quad (10)$$

The residual (10) is then nothing else that an optimal estimation of the fault, i.e.

$$r(k) = \hat{f}(k) = H_f r_f(k) \quad (11)$$

We also define two Schur polynomials D_{df} and A_{df} given from the following spectral factorization:

$$\begin{aligned} D_{df} D_{df}^* &= \tilde{C}_f \tilde{C}_f^* + \tilde{D}_s \tilde{D}_s^* \\ A_{df}^{-1} \begin{bmatrix} \tilde{C}_f \\ \tilde{D}_s \end{bmatrix} &= \begin{bmatrix} A_f^{-1} C_f \\ A_s^{-1} D_s \end{bmatrix} \end{aligned} \quad (12)$$

3.2. H_2 polynomial detection filter

The optimal detection filter H_f is required to minimize the following criterion:

$$J_{f_2} = \frac{1}{2\pi j} \oint_{|z|=1} (W_p \Phi_{e_f e_f} W_p^*) \frac{dz}{z} \quad (13)$$

where $\Phi_{e_f e_f}$ is the power spectral density of the fault

estimation error signal and $W_p = A_p^{-1} B_p$ a dynamic weighting function, which will improve the robustness of the detection.

Theorem 1: The optimal H_2 detection filter for the system defined by Fig. 2, and designed to minimize the cost function (13), is given by

$$H_f = (A_f^{-1} G_0 + B_p^{-1} N_0) D_{df}^{-1} A_{df}$$

where

- (G_0, S_0, F_0) denotes the minimal degree solution with respect to F_0 , of the following diophantine equation:

$$G_0 D_{df}^* z^{-g} + A_f F_0 = C_f \tilde{C}_f^* z^{-g}$$

- (N_0, F_{10}) , denotes the minimal degree solution with respect to F_{10} , of the following diophantine equation:

$$N_0 D_{df}^* z^{-g} + A_p F_{10} = B_p F_0$$

Proof: Derived by Mechbal (1999) from the result of Grimble (1993) ■

3.3. H_∞ polynomial detection filter

As mentioned in Section 2, the H_∞ detection filter will not minimize the variance error but the magnitude of the estimation error spectrum. The cost function is given by

$$J_{f_\infty} = \sup_{|z|=1} (W_p \Phi_{e_f e_f} W_p^*) \quad (14)$$

The optimal estimator is then obtained using an embedding procedure. Indeed, since H_∞ is a subspace of H_2 , it is possible to put the H_∞ estimation in an H_2 framework (see, Grimble *et al.*, 1989).

Theorem 2: The optimal H_∞ detection filter for the system defined by Fig. 2, and designed to minimize the cost function (14), is given by:

$$H_f = (A_f^{-1} G_0 + \bar{B}_\lambda^{-1} N_0) D_{df}^{-1} A_{df}$$

where

- (G_0, S_0, F_0) denotes the minimal degree solution with respect to F_0 , of the following diophantine equation:

$$G_0 D_{df}^* z^{-g} + A_f F_0 = C_f \tilde{C}_f^* z^{-g}$$

- (N_0, F_{11}) , denotes the minimal degree solution with respect to F_{11} , of the following diophantine equation:

$$N_0 D_{df}^* z^{-g} + \bar{A}_\lambda F_{11} = \bar{B}_\lambda F_0$$

- The polynomials \bar{A}_λ and \bar{B}_λ are given by:

$$\bar{A}_\lambda = A_\lambda A_p, \quad \bar{B}_\lambda = F_{0s} B_\lambda B_p$$

with A_λ and B_λ obtained from

$$A_\lambda A_\lambda^* = \lambda^2 (A_p A_p^* D_{df} D_{df}^* - B_p B_p^* C_f C_f^* D_s D_s^* / \lambda^2)$$

$$B_\lambda B_\lambda^* = A_p A_p^* D_{df} D_{df}^*$$

and the Schur polynomial F_{0s} is defined by:

$$F_{0s} F_{0s}^* = F_0 F_0^*$$

- The optimal function is: $J_{\min} = \lambda^2$.

Proof: Obtained by Mechbal (1999) from the result of Grimble (1993). ■

3.4. Robust evaluation

In the nominal case, and with a specific evaluation function, thresholds are generated. For the uncertain system, the problem is solved by using robust fault estimator and adaptive thresholds. For more details on this approach please refer to Mechbal and Vergé (2001).

4. EXPERIMENTAL SETUP

The mechanical structure is made of a composite beam with 3 pairs of piezoelectric ceramics bounded symmetrically to the vertical beam and covered by very thin electrodes on their top and bottom sides. The beam is constituted of two external thin plates between which is inserted a composite filling, as illustrated in Fig. 3. The actuators and sensors are PZ29 piezoelectric ceramics. The composite element is realized with pre-impregnated plies of composite material of reference 07628 ES15. The setup is completed by a control loop: charge and tension amplifiers and a specialized Dspace© card performing the real-time measurements, FDI and control.

4.1. FE modelling and Nastran simulations

Formulation of piezoelectric elements

In the following model formulation, we assume that the piezoelectric patches are perfectly bounded to the plate and the elastic electric fields are coupled.

FE equations for piezoelectric materials have already been formulated in many papers (Bruant *et al.* 1999). The linear constitutive relations for the direct and the inverse piezoelectric effects can be written as

$$\underline{\mathcal{E}} = \underline{S}^E \underline{\sigma} - \underline{d}^T \underline{E} \quad , \quad \underline{D} = \underline{d} \underline{\sigma} + \underline{\varepsilon}^\sigma \underline{E}$$

where the superscript T denotes a matrix transpose, $\underline{\mathcal{E}}$ is the vector of strain tensor components, $\underline{\sigma}$ is the vector of stress tensor components, \underline{D} is the electric displacement vector, \underline{E} is the electric field vector, \underline{S}^E is the elastic flexibility matrix evaluated at constant \underline{E} , \underline{d} is the piezoelectric coupling matrix and $\underline{\varepsilon}^\sigma$ is the dielectric matrix at constant stress. These equations can also be written in as,

$$\underline{\sigma} = \underline{C}^E \underline{\mathcal{E}} - \underline{e}^T \underline{E} \quad ,$$

$$\underline{D} = \underline{e} \underline{\mathcal{E}} + \underline{\varepsilon}^\varepsilon \underline{E} \quad \text{and} \quad \underline{\sigma} = \underline{C}^E \underline{\mathcal{E}} - \underline{e}^T \underline{E}$$

where $\underline{\varepsilon}^\varepsilon$ is the dielectric matrix at constant strain and \underline{C}^E is the elastic stiffness matrix evaluated at constant \underline{E} .

State representation and model reduction

Piezoceramics are discretized by mean of plate elements in order to model their mass and rigidity. The coupling is then introduced in the FE model that leads to the following equation (Bruant *et al.* 1999):

$$\underline{Q} = \underline{Q}_{ext} + \underline{Q}_a u(t)$$

where \underline{Q}_{ext} represents external mechanical strength and $\underline{Q}_a \cdot u$ represents actuator's effects. $u(t)$ is the input voltage. By duality, the characterization of the piezoelectric direct effect leads to a relation between the output voltage $y(t)$ and a function of the vector of mechanical nodal displacement:

$$y(t) = \underline{Q}_c q(t)$$

Now, using the previous FE model and taking into account a disturbance input, with form

$$\underline{Q}_{ext} = \underline{Q}_d d(t)$$

the equation of the motion of the structure becomes,

$$M \ddot{q} + C \dot{q} + K q = \underline{Q}_a u + \underline{Q}_d d$$

Defining the mode shape $\underline{\Phi}_i$ and the angular frequency ω_i of the i^{th} mode as the solution of the following generalized eigenproblem:

$$K \underline{\Phi}_i = \omega_i^2 M \underline{\Phi}_i$$

there exist then N linearly such $\underline{\Phi}_i$ where N is the size of the system. A reduction is done by projection of the nodal displacements on a truncated modal matrix. Let $\underline{\Phi}$ be this modal matrix and \underline{g} the vector of the associated generalized displacements defined by:

$$\underline{\Phi} = [\underline{\Phi}_1 \quad \dots \quad \underline{\Phi}_n] \quad , \quad n \ll N \quad ; \quad \underline{q} = \underline{\Phi} \underline{g}$$

After some substitution and left multiplying by $\underline{\Phi}^T$ the equation of the motion can be rewritten as:

$$m \ddot{\underline{g}} + c \dot{\underline{g}} + k \underline{g} = \underline{\Phi}^T \underline{Q}$$

where m , c and k are diagonal matrices.

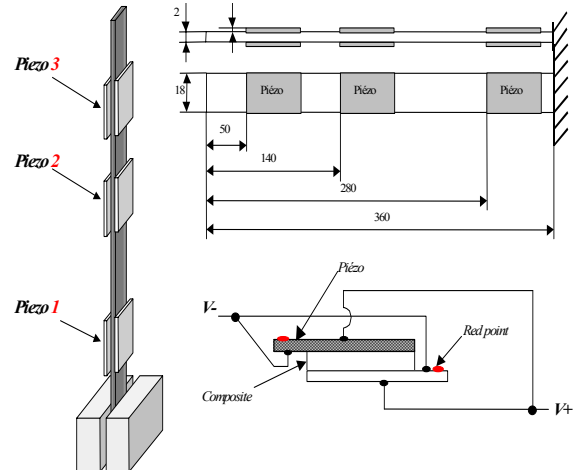


Fig. 3: The composite active structure.

The most important stage in the reduction of order is the choice of the eigenmodes kept in the reduced modal basis. Given the position of actuators and sensors, the modes are sorted regarding to their H_∞ norms as described in Henriot *et al.* (2000). By choosing now the state vector as:

$$\underline{x} = (\omega \underline{g}^T \quad \underline{\dot{g}}^T)^T, \quad (15)$$

we obtain a $2n$ order model that we turn into state space representation as:

$$\dot{\underline{x}} = \begin{bmatrix} 0_{n,n} & \text{diag}(\omega_i) \\ -\text{diag}(\omega_i) & -2\text{diag}(\zeta_i \omega_i) \end{bmatrix} \underline{x} + \begin{bmatrix} 0_{n,1} \\ \Phi^T \underline{Q}_a \end{bmatrix} u + \begin{bmatrix} 0_{n,1} \\ \Phi^T \underline{Q}_d \end{bmatrix} \zeta$$

$$y = [Q_c \cdot \Phi \cdot \text{diag}(1/\omega_i) \quad 0_{1,n}] \underline{x}$$

Then we can obtain the transfer functions of the process and the perturbation. It's a minimum phase plant where, for each transfer function, the first 3 modes were retained.

Actuator and sensor simulation

The FE model has been built with *Nastran*© software. However, this software does not contain any specific elements dealing with the piezoelectric coupling problem. So, we have elaborated an original strategy of simulation that consists in exploiting the analogy between thermal and piezoelectric equations. *Nastran* then, allows performing classical linear dynamical analyze. For details, see Mechbal (2005).

4.2. Experimental statements and FE updating

With the available actuators and sensors of the beam, we have access to necessary information for its identification. We obtain experimental Bode diagrams for each transfer between a sensor and an actuator. Indeed, as the beam is endowed with 3 sensors/actuators, it is therefore possible to define several couples (or path) of sensor/actuator (Fig. 3). Thus, the path 1-2 is represented by the transfer between actuator 1 and the sensor 2 (see, Fig. 4.)

In our framework, we compare the Bode diagram of different paths obtained by the FE model to those obtained by the experimental identification. Hence, we observe that differences are essentially due to DC gain (owing to amplifiers), which shows the validity of our FE model (Mechbal, 2005).

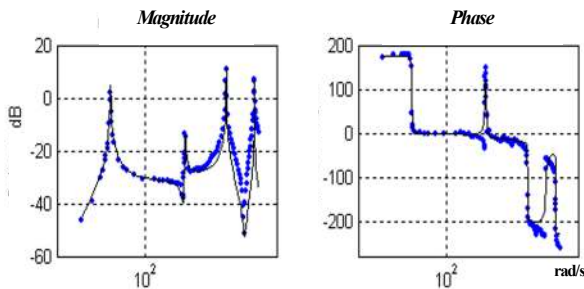


Fig. 4: Actual and simulated Bode diagrams for path 1-2.

4.3. Necessity of fault detection

The use of piezoelectric device as sensor or actuator can lead to different kind of failure:

- Cracks can appear in the ceramics,
- Ceramics can be poorly pasted,
- Stressed ceramics due to exposition to a high magnetic field.

If a ceramics is partially detached, the locally physical characteristics of the structure change which implies in addition to faulty measures an alteration of the global behavior of the structure. In the case of occurrence of cracks on ceramics, the global behavior of the structure is not modified but the useful surface of the ceramic is reduced. This kind of faults presents two consequences: a diminution of the gain and a lost of the symmetry of the setting.

4.4. Experiments

Here, we use as actuator the piezoceramic 1 and as sensors piezoceramic 2. The piezoceramic 3 creates the permanent disturbance. Noise has been measured on the structure. It is a white noise of variance of $2.58 \cdot 10^{-6} \text{ V}^2$. Hence, $A_b = B_b = 1$.

Robust H_∞ Regulator

To reject disturbances, we used a robust H_∞ controller.

To elaborate it we used the reduced model based on the first 3 modes of the identified one (see Fig. 4). We have also defined multiplicative uncertainty on the output that represent neglected dynamics. The controller has been applied to the actual process at 1s. For a permanent perturbation of a frequency of 6.3Hz (Fig.5.), we can notice that the settling-time is strongly decreased.

Fault estimation

Several tests have been performed. Faults are described as changes in sensor gain and to model them, we choose a low pass weight function given by

$$W_f = \frac{0.00044z^{-1}}{1 - 0.9998z^{-1}}$$

The function $1/W_p$ was taken as an integrator to emphasize the signal in low frequency.

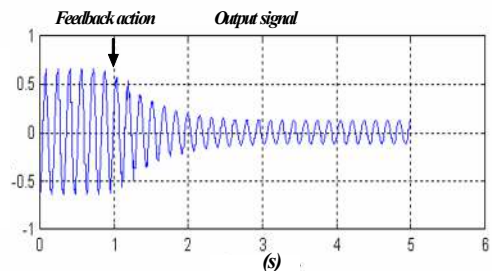


Fig. 5: Actual output signal with H_∞ controller

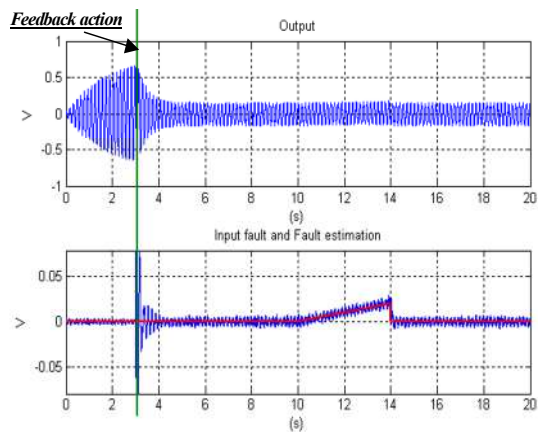


Fig. 6: Output and fault estimation for $f = 6.3$ Hz: Sensor fault – ramp of slope 0.008.

We present here results related to different sensor faults with the H_∞ estimator:

Small Drift fault: Here the gain of the sensor is increased as a ramp function entering from $t = 10s$ to $t = 14s$ with a slope of 0.008. It's a small fault that represents a drift of the piezoelectric gain. Fig.6. indicates that is not possible to detect the fault using only the measure of the output. Of course, performing detection by analyzing only the output depends on the kind and the magnitude of faults. But, without integrating FD procedure, it is hard to make distinction between fault and perturbation or noise effect. In addition to that, controller could mask the fault effect on the output because it interprets the fault as a perturbation and would try to reject it.

Small Step fault: the simulated fault is described as a step function of amplitude 0.02 V. Fig.7. shows that the estimation is quite fast but not very accurate. This is due to the fact that we want to detect small fault in the presence of noise measure.

Robustness test: we performed simulations where the controller and estimator have been calculated on the basis of the identified model but the simulations have been performed with a model in which the modal frequencies have been modified. Fig.8. shows that the controller and the estimator give good results in spite of the presence of uncertainties and noise.

5. CONCLUSION

This paper described the design of an active robust fault estimation scheme. The experimental set up is a structure made of a composite beam with piezoelectric patches. This work focuses on the necessity of including FDD procedure in any active control strategy to ensure safe applications.

The proposed approach, using polynomial H_2/H_∞ estimation, is an original method to solve the robust fault detection problem. It gives satisfactory results.

Further, works are under study and experiments on the actual process are in progress.

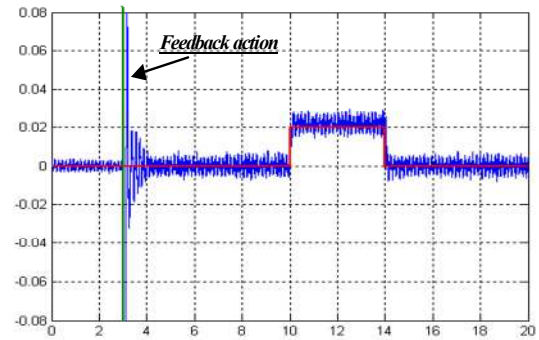


Fig. 7: Output and fault estimation for $f = 6.3$ Hz: Sensor fault – step of 0.02V.

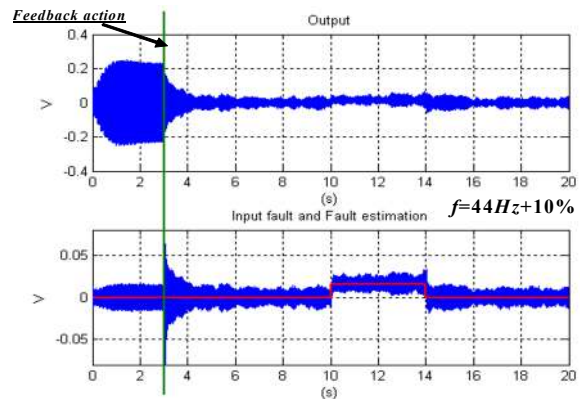


Fig. 8: Output and fault estimation for $f = 44$ Hz+10%: Sensor fault – step of 0.02V.

REFERENCES

- Bruant I., G. Coffignal, F. Léné and M. Vergé (1999). A methodology for determination of piezoelectric actuators and sensors geometry on beams structures". *Journal of Sound and Vibration*, vol 219, (5), 1999.
- Gawronski. W.K. (1998), *Dynamics and control of structures, a modal approach*, Springer.
- Grimble, M.J, Ho, D. & Elsayed, A. (1989). H_∞ robust linear estimator, *IFAC Adaptive Systems in Control and Signal processing*, Glasgow, pp. 477-481.
- Grimble, M.J. (1993). *Robust Industrial Control: Optimal Design Approach for Polynomial Systems*, Prentice Hall international.
- Henriot P., M. Vergé. and G. Coffignal (2000). Model reduction for active vibration control. *SPIE's 7th Annual International Symposium on Smart Structures and Materials*, California, USA.
- Iserman, R. (2005). Model Based fault detection and diagnostic – status and applications. *Annual reviews in control, Elsevier* **29**, pp71-85.
- Kwakernaak H. (1986). A polynomial approach to minmax frequency domain optimization of multivariable feedback systems. *Int. J. Control*, Vol. **44**, pp. 117-156.
- Mechbal N. (2005). Simulations and Experiments on Active Vibration Control of a Composite Beam with Integrated Piezoceramics. IMACS, Paris.
- Mechbal, N. (1999). Détection Robuste de Défauts par Approche polynomiale, Phd thesis, ENSAM, Paris.
- Mechbal, N. and M. Vergé. (2001). An Approach to Optimally Robust Fault Detection and diagnosis. *CCA 2001*, Mexico.
- Mechbal, N., Guillard, H. & Vergé, M. (2000). An approach to the robust fault detection for uncertain systems with time varying parameters., *SAFEPROCESS'2000*, Budapest, pp.485-490.